SCIENCE CHINA
Earth Sciences

• RESEARCH PAPER •

doi: 10.1007/s11430-015-0192-1

Improved data gap-filling schemes for estimation of net ecosystem exchange in typical East-Asian croplands

ZHAO Peng[1,2*] & Johannes LÜERS[1,3]

[1] *Department of Micrometeorology, University of Bayreuth, Universitätsstrasse 30, 95447, Germany;*
[2] *Institute of Ecology, University of Innsbruck, Sternwartestraße 15, 6020, Austria;*
[3] *Member of Bayreuth Center of Ecology and Environmental Research (BayCEER), University of Bayreuth, Bayreuth 95540, Germany*

Received November 29, 2015; accepted February 16, 2016

Abstract The estimation of carbon exchange between ecosystems and the atmosphere suffers unavoidable data gaps in eddy-covariance technique, especially for short-living and fast-growing croplands. In this study we developed a modified gap-filling scheme introducing a leaf area index factor as the vegetation status information based on the conventional light response function for two East-Asian cropland sites (rice and potatoes). This scheme's performance is comparable to the conventional time window scheme, but has the advantage when the gaps are large compared to the total length of the time series. To investigate how the time binning approach performs for fast-growing croplands, we tested different widths of the time window, showing that a four-day window for the potato field and an eight-day time window for the rice field perform the best. The insufficiency of the conventional temperature binning approach was explained as well as the influence of vapor pressure deficit. We found that vapor pressure deficit plays a minor role in both the potato and the rice fields under Asian monsoon weather conditions with the exception of the early pre-monsoon growing stage of the potatoes. Consequently, we recommend using the conventional time-window scheme together with our new leaf-light response function to fill data gaps of net ecosystem exchange in fast-growing croplands.

Keywords Eddy-covariance, Gap-filling, Net ecosystem exchange, LAI

Citation: Zhao P, Lüers J. 2016. Improved data gap-filling schemes for estimation of net ecosystem exchange in typical East-Asian croplands. Science China Earth Sciences, doi: 10.1007/s11430-015-0192-1

1. Introduction

Contemporary cultivated areas comprise 24% of the terrestrial surface of the earth (Millennium Ecosystem Assessment, 2005). The estimate for net ecosystem exchange (NEE) of carbon dioxide (CO_2) in croplands is therefore an important issue for the study on global carbon budget. The eddy-covariance technique is well-known for the ability to continuously and directly quantify NEE between the earth surface and atmosphere (Baldocchi et al., 2001; Baldocchi, 2003). However, data gaps in the eddy-covariance technique are unavoidable and limit the carbon budget estimate. An average of 35% of flux observations are reported as missing or rejected (Falge et al., 2001). Data gaps are due to system breakdown, calibration, and maintenance, or caused by farming or human activities, or by weather conditions when the assumptions required by the eddy-covariance technique are not fulfilled (Foken and Wichura, 1996). The incompleteness of datasets requires gap-filling and correcting strategies based on the understanding of ecosystem-atmosphere exchange (Papale, 2012).

The gap-filling strategies for NEE data have drawn much attention in the last decade. Many statistical and empirical approaches have been developed and discussed considering the major driving factors for NEE, i.e. the growing stages of the vegetation of interest, the light response of the plant,

* Corresponding author (email: peng.zhao@uibk.ac.at)

air or soil temperature, vapor pressure deficit (VPD), and soil water availability (Greco and Baldocchi, 1996; Falge et al., 2001). Amongst all of these, mean diurnal variation, look-up table, and non-linear regression are the most commonly used methods. New gap-filling methods have been developed, including dual unscented Kalman filter (Gove and Hollinger, 2006), artificial neural networks (Papale and Valentini, 2003), multiple imputation method (Hui et al., 2004), and other biosphere energy-transfer hydrology models (Moffat et al., 2007). However, these methods are evaluated for European and American sites rather than Asian ones. Moreover, these studies are mainly related to forests rather than fast-growing crops.

Compared to forest ecosystems, a cropland ecosystem has the special features and requires different considerations to estimate NEE and to deal with data gaps. Most of the available papers do not mention the leaf area index (LAI), or just treat LAI as a constant in time, probably because the LAI of forests is large and the change of LAI is too small to detect with remote sensing techniques. However, the cropland canopy changes rapidly during the growing season. Gaps in these fast growing stages could introduce more uncertainty than slow-growing stages (Richardson and Hollinger, 2007). Some of the conventional gap-filling strategies (e.g. mean diurnal variation, look-up tables, and non-linear regression) are normally based on monthly or even seasonal time windows. To take into account a rapid LAI change, time windows as short as a few days (Ammann et al., 2007) are needed to capture the rapid change in the CO_2 exchange. This could enlarge the problem that the minimum number of data, which are needed in each time window to apply the statistics, is not reached. An additional problem is that many crops have growing seasons as short as three or four months, resulting in a database less sufficient than evergreen forests for some gap-filling strategies such as artificial neural networks, which need large data-sets for training. Moreover, croplands are so intensively managed and manipulated by farmers' decisions (e.g. irrigation, different planting and harvesting dates) across both regions and time (Li et al., 2011) that it is difficult to find a universal strategy encompassing the site-specific year-to-year variation. Croplands are usually patchy with a mixture of crop species, which results in mixed NEE information captured by the eddy-covariance technique. Footprint heterogeneity should be included to improve the performance of parameterization routines (Falge et al., 2001). Seasonal weather patterns increase the complexity of gap-filling as well. For instance, the monsoon is a major factor strongly controlling the carbon budget in Asia (Kwon et al., 2010). Intensive rain, snow or storm events disturb the eddy-covariance measurements resulting in large periods without reliable observations. Furthermore, filling large gaps provides more challenge than small gaps because the change of the canopy and the underlying surface properties with time must be considered (Falge et al., 2001; Moffat et al., 2007; Richardson and Hollinger, 2007). Further investigations on croplands have been requested, and other factors such as physiological factors are required to validate and improve the gap-filling methods (Falge et al., 2001; Moffat et al., 2007; Xing et al., 2007).

The information about NEE of croplands is limited (Falge et al., 2002) due to the lack of researches focused on this topic especially in Asia. Recently, Lei and Yang (2010) have reported seasonal and inter-annual variations in NEE at a winter wheat/summer maize rotation cropping site in the North China Plain. Du and Liu (2013) have reported seasonal and inter-annual variation of NEE in a maize cropland in a semi-arid area of China. Eddy-covariance technique was used in both studies. Lindner et al. (2015) have studied seasonal patterns of NEE in five croplands (potato, rice, radish, cabbage, and bean) in Korea, using a closed chamber system. None of these studies has focused on the development of gap-filling methods for NEE data.

This study was intended to improve the gap-filling methods for NEE data collected in fast-growing croplands. We presented a modified parameterization approach, including a LAI factor as the information about the growing stages of fast-developing croplands in a simple and comparable way. An improved criterion for applying the data-binning methods with a statistical based approach was investigated for the first time. The sensitivity of the conventional methods to different parameterization approaches was discussed as well.

2. Materials and methods

2.1 Data collection

We carried out the observation in the field campaign of the TERRECO (Complex TERRain and ECOlogical Heterogeneity) project at Haean Punchbow, Yanggu-gun, Kangwon-do, South Korea, in 2010. Haean Punchbow is an intensively-managed agricultural area surrounded by mountains and influenced by the Asian monsoon. We chose a potato field site (38°16′38″N, 128°7′28″E, 455 m a.s.l.) and a rice field site (38°17′28″N, 128°7′52″E, 457 m a.s.l.) for study. The growing seasons in 2010 lasted from the planting day of DOY 116 to the harvesting day of DOY 273 for potato (26 April to 30 September 2010), and DOY 144 (transplanting day) to DOY 290 (harvesting day) for rice (24 May to 17 October 2010). Normally potatoes are harvested at the end of August. However, intensive rain events during summer 2010 postponed the harvesting day to one month later than usual.

An eddy-covariance system was alternately running in the potato field or the nearby rice field for, in total, three periods at

each site. The first period at the potato site lasted from DOY 152 to 175, the second from DOY 187 to 203, and the last from DOY 225 to 240. In between, the eddy-covariance system was moved to the rice field site (from DOY 177 to 186, 203 to 223 and 242 to 274). The turbulence fluxes of CO_2 were measured on a mast 2.5 m above ground at the potato field and 2.8 m at the rice field, using an ultrasonic anemometer (USA-1, Meteorologische Messtechnik GmbH, Germany) and a fast-response open-path H_2O/CO_2 analyzer (LI-7500, LI-COR Inc., USA). The software package TK3 (Mauder and Foken, 2011) post-processed high frequency (20 Hz) raw data to calculate 30-min aggregated fluxes of NEE and generate the observed database (Database-observation). This flux calculating and correcting strategy is well documented, intercompared by the international micrometeorology community (Mauder et al., 2008), and successfully applied during known major field experiments such as EBEX-2000 (Mauder et al., 2007; Oncley et al., 2007), LITFASS-2003 (Mauder et al., 2006), and COPS-2007 (Eigenmann et al., 2011). Automatic weather stations (AWS, WS-GP1, Delta-T Devices Ltd., UK) were used at both sites for the measurement of meteorological variables (5-min values), including air temperature, humidity, wind speed and direction, precipitation, and global radiation. Biomass samples were collected and measured half-monthly at both sites. On each occasion, five to ten whole plants were randomly sampled and leaves were immediately separated and analyzed by a leaf area meter (LI-3000A, LI-COR Inc., USA) to calculate the LAI. A linear interpolation between the measured LAI values was used to produce a complete time series. For further information about the field campaign, see Zhao et al. (2011).

2.2 Generation of high-quality database

In order to examine time series of fluxes and generate a high-quality database, we applied the data-quality selection criteria by Lüers et al. (2014). Briefly speaking, TK3 eliminated spikes in 20-Hz records, and filtered direct measurements (e.g. horizontal wind speed, vertical wind speed after rotation, sonic temperature, absolute humidity, and carbon dioxide concentration) and subsequently derived variables (e.g. covariance, wind direction, atmospheric stability, and all fluxes) by applying reasonable physical consistency limits. An overall quality classification strategy (Foken and Wichura, 1996; Foken et al., 2004) combining steady-state test and the integral turbulence characteristics test marked the derived 30-min fluxes with overall quality flags of 7–9 as low-quality data, and marked the flux data with flags of 1–6 as high-quality data for further analysis. The diagnostic signals (i.e. AGC, the status of the chopper motor and the chopper temperature controller, the detector cooler, and the sync between the LI-7500 embedded software and the chopper motor) from LI-7500 digital outputs were used to mark those values during rain and fog events as outliers as well. Furthermore, the internal boundary layer and footprint information was used to estimate the contribution by the target surface. Turbulent flux data were marked as irrelevant records when flux contribution from the target land-use type was less than 70% and the aerodynamic measurement height was larger than $0.5x^{0.5}$ (Eigenmann et al., 2011), where x is the fetch. Finally, a statistical algorithm check, including an absolute deviations filter and a standard deviation filter, was performed on the basis of the comparison between each 30-min value and the values before and after. Database-observation excluding low quality data and outliers by the steps above was used as the high-quality database (Database-high-quality).

The final data coverage of Database-high-quality is 71% for the potato field and 59% for the rice field during the measurement periods. For the potato field, the data gaps cover 1% because of the power failure, 21% by the AGC-check, 3% by eliminating low-quality classified data, and 4% by applying the statistical outlier check. For the rice field, this distribution is only slightly different (7%, 30%, 2%, and 2%, respectively).

2.3 Gap-filling methods

2.3.1 *Database for gap-filling*

NEE of Database-high-quality was partitioned into ecosystem respiration (R_{eco}) and gross primary productivity (GPP):

$$\mathrm{NEE} = \mathrm{GPP} + R_{\mathrm{eco}}. \quad (1)$$

The signs follow the conventional meteorological definitions that carbon uptake by the ecosystem is negative and carbon release is positive.

Assuming no photosynthesis during nighttime (Reichstein et al., 2005), the measured nighttime NEE is equal to R_{eco}. Thus, the night-time NEE was used for the parameterization R_{eco} (Section 2.3.2). The fitted parameters and daytime temperature were used to calculate the daytime R_{eco}. GPP was obtained by subtracting R_{eco} from NEE and then used for evaluation of the gap-filling schemes. The separation of data into daytime data and nighttime was performed by the evaluation of global radiation with a threshold of 20 W m^{-2} and cross-checked against sunrise and sunset time derived from the local time and standard sun-geometrical routines (Reichstein et al., 2005; Papale et al., 2006; Lasslop et al., 2010).

2.3.2 *R_{eco} estimate*

The Lloyd-Taylor function (Lloyd and Taylor, 1994; Falge et al., 2001; Ruppert et al., 2006) was used for parameterizing the temperature dependence of R_{eco}:

$$R_{\mathrm{eco}} = R_{\mathrm{ref}} e^{E_0\left(\frac{1}{T_{\mathrm{ref}} - T_0} - \frac{1}{T - T_0}\right)}, \quad (2)$$

where R_{ref} (μmol m^{-2} s^{-1}) is the ecosystem respiration rate at

a reference temperature (T_{ref}, set as 283.15 K), E_0 (K) is the temperature sensitivity, T (K) is the air temperature, and T_0 (K) is a constant value of 227.13 K as in Lloyd and Taylor (1994).

2.3.3 *Parameterization for the light response function*

(1) Conventional schemes (temperature or time-window binning scheme). Light response functions describe the solar radiation dependency of NEE. As the rectangular hyperbolic function shows the best overall performance among many light response functions used for daytime NEE gap-filling (Falge et al., 2001), the gap-filling methods in this study are on the basis of the Michaelis-Menten function (Michaelis and Menten, 1913)

$$\mathrm{NEE}=\frac{\alpha R_g \beta}{\alpha R_g+\beta}+R_{eco}, \tag{3}$$

where R_g (W m^{-2}) is the global radiation, α (μmol s^{-1} W^{-1}) is the initial slope of the curve, and β (μmol m^{-2} s^{-1}) is the saturated CO_2 uptake rate when R_g is close to infinity.

It has been reported that the parameterization for eq. (3) can be improved by a temperature binning scheme (binning observations into temperature classes) to capture the temperature dependence of the carbon assimilation (Falge et al., 2001; Ruppert et al., 2006), or by a time-window scheme (binning observations into time intervals) to distinguish different seasonal response within different periods (Falge et al., 2001; Moffat et al., 2007). Different opinions, however, exist in the community about the utilization of these schemes. The temperature binning scheme is based on the fact that the assimilation of CO_2 has an optimal temperature, below or above which the photosynthesis ability will decrease (Saxe et al., 2001). Nevertheless, it was found that air temperature has weak influence on photosynthesis during summer in forests (Bassow and Bazzaz, 1998). The time-window scheme is based on the seasonal changes in leaf area, soil moisture and photosynthetic capacity, which leads to the requirement of continual updating and adjusting of the regression scheme (Baldocchi, 2003). The selection of time windows was empirical and varying from one month to a full year for forest sites (Falge et al., 2001; Stoy et al., 2006; Moffat et al., 2007). For grassland, the use of a 5-d moving window to capture the rapid change of the surfaces was reported (Ammann et al., 2007). A short time window of 4 to 15 d was often used to account for seasonal parameter variability (Lasslop et al., 2010). Generally, the widths of time windows for regression depend on (1) how rapidly the vegetation develops, and (2) how large the gaps are because the time-window scheme cannot fill gaps larger than the selected time window (Falge et al., 2001; Stoy et al., 2006), which could be a problem for sites influenced by power failure or bad weather. It was reported, however, that additional temporal sub-binning of data did not significantly improve the simulation of temperature binning scheme for forest sites (Ruppert et al., 2006). In this study, Database-high-quality was binned into 14, 8, 4, or 2 K temperature classes, or sorted into 16, 8, 4, or 2 d time windows, to test the temperature and seasonal dependencies of the parameterization of eq. (3). Individual fittings of α and β were determined for each temperature class or time window.

A VPD factor was introduced to account for the stomatal response to dry air conditions. Eq. (3) was modified by introducing an exponential function (Lasslop et al., 2010)

$$\beta=\begin{cases}\beta_0 e^{-k(\mathrm{VPD}-\mathrm{VPD}_0)}, & \mathrm{VPD}>\mathrm{VPD}_0,\\ \beta_0, & \mathrm{VPD}\le \mathrm{VPD}_0,\end{cases} \tag{4}$$

where β_0 was a parameterized constant, and the threshold VPD_0 (hPa) was set to 10 hPa (Lasslop et al., 2010).

(2) Modified scheme (LAI factor scheme). As carbon exchange between agro-ecosystems and the atmosphere is strongly correlated to crop development (Béziat et al., 2009), and LAI plays a key role in the allocation of carbon to leaves (González-Sanpedro et al., 2008), our modified scheme for seasonal response introduces a LAI factor to account for seasonal variability.

Firstly, GPP is expressed as

$$\mathrm{GPP}=\frac{\alpha R_g \beta}{\alpha R_g+\beta}. \tag{5}$$

Suppose that each unit area of leaves which are active in photosynthesis has equal ability of carbon uptake. A leaf-light response function by introducing a LAI factor into eq. (5) is proposed as

$$\frac{\mathrm{GPP}}{\mathrm{LAI}_{act}}=\frac{\alpha' R_g \beta'}{\alpha' R_g+\beta'}, \tag{6}$$

or

$$\mathrm{GPP}=\mathrm{LAI}_{act}\frac{\alpha' R_g \beta'}{\alpha' R_g+\beta'}, \tag{7}$$

where LAI_{act} is the mean LAI which is active in photosynthesis, approximately taken as measured LAI in this study. The parameters α' and β' can be defined as specific light use efficiency and specific saturated GPP. We suppose that α' and β' are constant for a given crop species and do not change with the vegetation development. Therefore, the whole dataset of R_g, GPP, and LAI_{act} within the growing season can be used to parameterize eq. (7). Consequently, large gaps in GPP are expected to be filled with the derived parameters α' and β', because the non-linear development of LAI is already included.

The leaf-light response function (eq. (7)) is a combination of both leaf and light responses of GPP. The validation of eq. (7) was performed in three steps: firstly, the light response function (eq. (5)) is a special case of eq. (7) when the vegetation condition is constant. Thus, for a given value of LAI_{act},

the coefficient α and β in eq. (5) must hold constant. Secondly, for a given value of solar radiation, $\alpha\ 'R_g\beta'/\alpha'R_g+\beta'$ must be constant, thus a LAI response function can be expressed as

$$\mathrm{GPP}=a_{\mathrm{LAI}}\mathrm{LAI}_{\mathrm{act}}, \tag{8}$$

where a_{LAI} is a constant slope. Finally, the whole dataset must follow eq. (7).

2.3.4 *Evaluations of the methods*

To assess the agreement between the observation and the simulation by the fitted parameters, a random walk was performed along Database-high-quality to mark 10% of them as artificial gaps (Database-artificial-gaps) (Moffat et al., 2007). The remaining 90% of Database-high-quality were used to fit the equations of the models in question (Database-parameterization). The gap-filling methods were evaluated by examining the comparison between the simulation (Database-simulation) and Database-artificial-gaps. We evaluated the overall performance of these methods by ranking Nash-Sutcliffe model efficiency coefficient (NSeff; Legates and McCabe, 1999) and index of agreement (d) between Database-simulation and Database-artificial-gaps. Additionally, mean average error (MAE), standard deviation (SD), root mean square error (RMSE), and normalized root mean square error (NRMSE) were also calculated to indicate the magnitude and distribution of the individual errors.

We used Taylor diagrams (Taylor, 2001) to plot SD, R, and NRMSE of the agreement between Database-simulation and Database-artificial-gaps in one figure in order to test the sensitivity of a gap-filling scheme. In a Taylor diagram, each single point specifies the performance of one scheme, with the radial distance as SD, the polar angle as R, and distance to observation point as NRMSE. A farther distance between two simulations indicates a bigger sensitivity.

3. Results and discussion

3.1 Meteorological conditions and biomass development

The meteorological conditions and biomass development during the growing seasons are shown in Figure 1. As the research sites were located only 1.5 km away from each other without big obstacles in between, the daily meteorological conditions were quite similar. Therefore, only those at the potato field are shown. Daily mean temperatures at both sites varied from 8 to 27°C during the growing seasons. The warmest month was August with a monthly mean of 22°C. The daily mean relative humidity was often high, above 80%

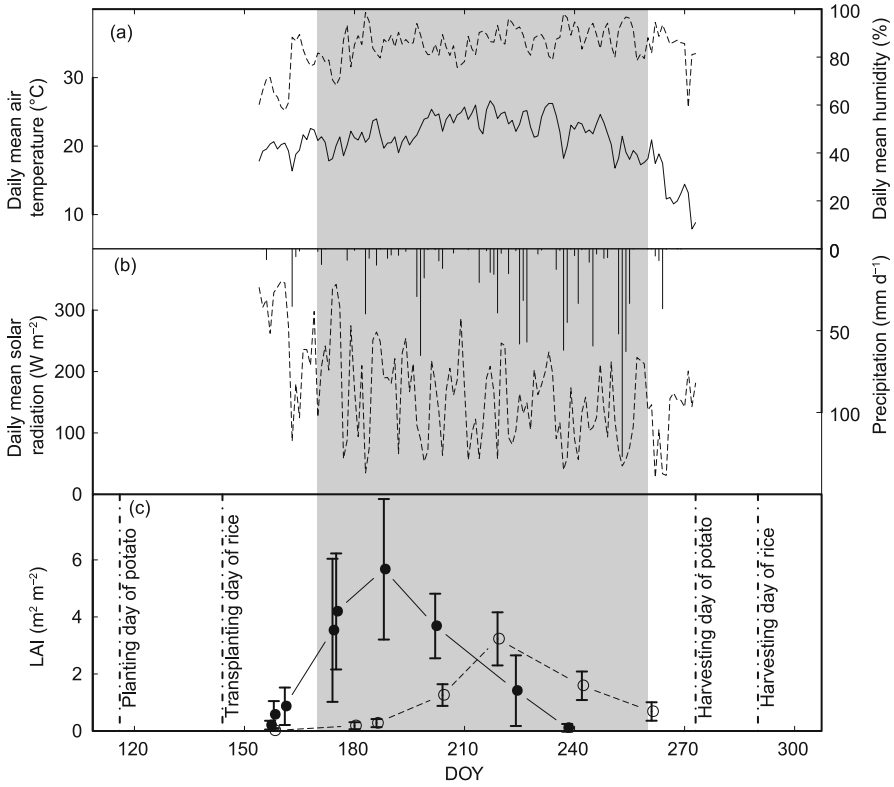

Figure 1 Meteorological conditions and biomass development at the research sites, including daily mean air temperature ((a), solid line), daily mean air relative humidity ((a), dashed line), daily sum precipitation ((b), bar), daily mean solar radiation ((b), dashed line), and leaf area index (LAI, (c), solid line representing potato and dashed line representing rice). Error bars are the standard deviations. The vertical dot lines from left to right indicate the planting day of potato, the transplanting day of rice, the harvesting day of potato, and the harvesting day of rice, respectively. The shaded area indicates monsoon and subsequent typhoon season.

on most days from June to August, resulting in many fog events. The annual precipitation was 1586 mm in 2010, close to the annual mean of 1577 mm over the last 11 yr. 75% of the annual precipitation fell in the crop growing season from June to September. However, the precipitation in June (70 mm) and July (222 mm) was only half of the 11 yr monthly mean, while the precipitation in September (427 mm) was more than twice the 11 yr monthly mean, indicating a time shift of the summer monsoon. Large gaps (several days) in Database-parameterization were found during these rain events because of the poor instrument status.

LAI changed rapidly at both sites. In the rice field, the plants had a LAI close to zero at the beginning of the initial stage. Leaves and stems grew rapidly in the development stage, when a maximum increasing rate of LAI reached 0.24 m^2 m^{-2} per day in late July. From the beginning of the mid-season, the grains emerged and grew fast with the decrease of green leaves until the late-season. The potato started a rapid growth in the development stage, with the LAI increasing from 0.5 to 4 m^2 m^{-2} within just one month. The maximum growing rate of LAI reached 0.21 m^2 m^{-2} per day in June. In the following mid- and late-seasons, the new tubers grew while green leaves declined. At the end of the growing season, almost all green leaves disappeared. The harvest of potatoes typically took place in late August or early September only if the field was dry enough. In 2010, however, the intensive rainfall in August led to too wet and heavy soils until the end of September. Therefore, the late potato season in 2010 was longer than in normal years.

3.2 Conventional time-window scheme

The performances of simulations applying the conventional time-window scheme for daytime NEE simulation are shown in Figure 2 and Table 1. The time-window scheme apparently improves the agreement between the simulation and the observation, with high indexes of agreements (d) up to 0.98 and NSeff up to 0.93. No difference in sensitivity between the time windows of 8, 4, and 2 d is found either in Figure 2 and Table 1, or by d, or NSeff. If the width of the time window increases above a certain length (more than 16 d in this study) the performance decreases significantly. For the potato field, the mean average error is 2.2 μmol m^{-2} s^{-1} (8 d), 1.9 μmol m^{-2} s^{-1} (4 d), and 1.9 μmol m^{-2} s^{-1} (2 d). Therefore, a 4 d time window is as good as a 2 d and better than an 8 d window. For the rice field, 8, 4 and 2 d time windows perform similarly, with identical mean average errors of 1.6 μmol m^{-2} s^{-1}. The 2 d time window performs even a little worse than the 4 d time window at the rice field because of the insufficient data coverage. Therefore, the best time window is 4 d for the potato field and 8 d for the rice field. If we consider the mean change rate of LAI, we find that the change in LAI (ΔLAI) within these optimal time windows is approximately 0.5 m^2 m^{-2}. The simulations are not sensitive to the widths of time windows when ΔLAI<0.5 m^2 m^{-2}. Therefore, this value of ΔLAI could be used as an indicator to determine the width of the best time windows for inter-site comparison and even for other types of croplands.

3.3 Performance of LAI-factor scheme

We picked observations with several constant values of LAI (1, 2, 4 m^2 m^{-2} with a tolerance window of ±0.1 m^2 m^{-2}) out of the high quality database as the first step to validate the LAI-factor scheme. For each group with a constant LAI, the non-linear-regression was applied to parameterize the light-response function (eq. (5)). The model for each constant LAI value had small standard error (SE) of 0.009 to 0.017 μmol s^{-1} W^{-1} for α, and 2 to 12 μmol m^{-2} s^{-1} for β, which demonstrated that α and β hold nearly constant for a give value of LAI. Moreover, the absolute value of α increased from 0.041 to 0.101 μmol s^{-1} W^{-1} and β from 16 to 57 μmol m^{-2} s^{-1} with the increase of LAI from 1 to 4 m^2 m^{-2}, which indicated that the values of both α and β were influenced by LAI values.

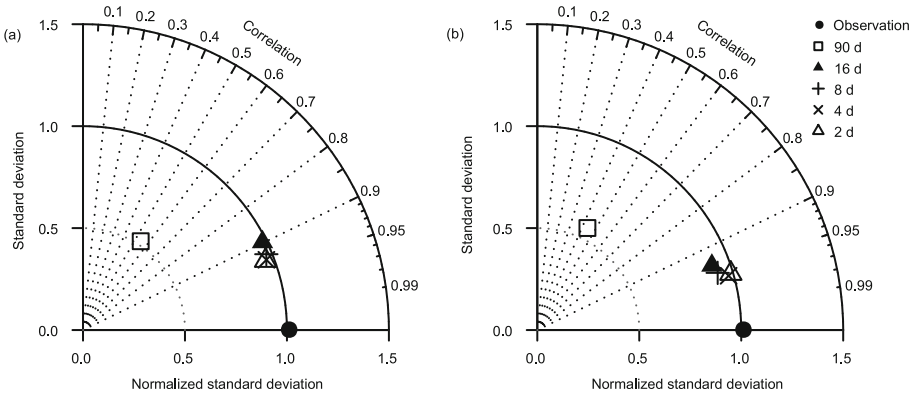

Figure 2 Taylor diagrams for the performances of simulations applying the time-window scheme and the LAI-factor scheme at the potato field (a) and the rice field (b). The polar radial distance is the normalized standard deviation (NSD). The polar angle is the correlation coefficient (R).

Table 1 Comparison between the simulation and observation of net ecosystem exchange of carbon dioxide

Scheme	Potato					Rice				
	MAE	RMSE	rSD	*d*	*R*	MAE	RMSE	rSD	*d*	*R*
Temperature binning 28 K	4.8	6.2	0.52	0.66	0.55	6.0	7.5	0.56	0.61	0.44
Temperature binning 14 K	4.8	6.2	0.52	0.66	0.55	4.9	6.4	0.64	0.75	0.63
Temperature binning 8 K	4.8	6.2	0.62	0.70	0.55	4.0	5.3	0.72	0.85	0.77
Temperature binning 4 K	4.7	6.1	0.64	0.72	0.58	3.7	5.0	0.73	0.87	0.80
Temperature binning 2 K	4.5	6.1	0.66	0.72	0.57	3.8	5.0	0.74	0.87	0.79
Time window 90 d	4.8	6.2	0.52	0.66	0.55	6.0	7.5	0.56	0.61	0.44
Time window 16 d	2.6	3.3	0.97	0.95	0.90	1.9	2.9	0.91	0.97	0.94
Time window 8 d	2.2	2.9	0.97	0.96	0.93	1.6	2.5	0.93	0.97	0.95
Time window 4 d	1.9	2.6	0.96	0.97	0.93	1.6	2.2	0.98	0.98	0.96
Time window 2 d	1.9	2.6	0.95	0.97	0.94	1.6	2.3	0.99	0.98	0.96
LAI-factor	3.0	4.3	1.23	0.93	0.88	5.2	6.6	1.42	0.88	0.85

The second step to validate the LAI-factor scheme was performed in a similar way: observations with several constant values of solar radiation (100, 200, 400, 600 W m^{-2} with a tolerance window of ±20 W m^{-2}) were picked out of the high quality database. For each group with a constant solar radiation, the linear regression between GPP and LAI was applied (eq. (7)). GPP showed good correlation (R^2 ranging between 0.87 to 0.95, standard error of the slope a_{LAI} ranging between 0.09 to 0.30 μmol m^{-2} s^{-1}) for a given value of solar radiation, which demonstrated that the LAI response function (eq. (8)) holds. Furthermore, the absolute value of the linear slope a_{LAI} increases from 2.08 to 6.52 μmol m^{-2} s^{-1} with the increase of solar radiation from 100 to 600 W m^{-2}, indicating the influence of solar radiation on a_{LAI}.

The mixed influence of both LAI and solar radiation could already be seen in the first and second steps, which resulted consequently in the third step. The non-linear regression of the leaf-light response function (eq. (6)) was applied to the whole high quality dataset. The modeled values of α' are −0.039 μmol s^{-1} W^{-1} for potato and −0.024 μmol s^{-1} W^{-1} for rice, while the values of β' are −15.6 μmol m^{-2} s^{-1} for potato and −11.5 μmol m^{-2} s^{-1} for rice. α' is 63% larger, and β' is 36% larger in the potato field than in the rice field, indicating that potato has a more robust ability of carbon assimilation than rice on the basis of unit LAI. The leaf-light response of GPP can be seen in Figure 3. For a given LAI, eq. (6) becomes the conventional light response function (eq. (5)). For a given solar radiation, eq. (6) becomes the LAI response function (eq. (7)).

A good agreement between the simulated GPP by the leaf-light response function and the derived GPP from the observed NEE and simulated respiration was found. The linear regression showed R^2 of 0.85, slope of 1.00±0.01, and intercept of 1.38±0.18 μmol m^{-2} s^{-1} for the potato field, and R^2 of 0.72, slope of 1.02±0.02, and intercept of 3.44±0.33 μmol m^{-2} s^{-1} for the rice field. The index of agreement (*d*) confirmed the reliability of the simulation with 0.93 for the potato field and 0.88 for the rice field as well. This good performance of the leaf-light response function indicates that it could be used to parameterize the light response of crops as an alternative method to the time-window scheme to capture the seasonal change of the vegetation and surface conditions.

The validation of the leaf-light response function provides evidence to explain the relationship between the light use efficiency (α) and LAI reported in the literature. It was found that the light use efficiency increases with development of a crop (Suyker et al., 2005). Positive correlation between *a* and LAI with R^2 = 0.83–0.93 was reported for grass component of a fen ecosystem (Otieno et al., 2009) and with R^2 = 0.40–0.98 for a variety of crops (Lindner et al., 2015). In our study, comparing eqs. (5) and (7) can derive α=$LAI_{act}\alpha'$ and β=$LAI_{act}\beta'$, indicating that the constant α' (or β') is the slope of the lin-

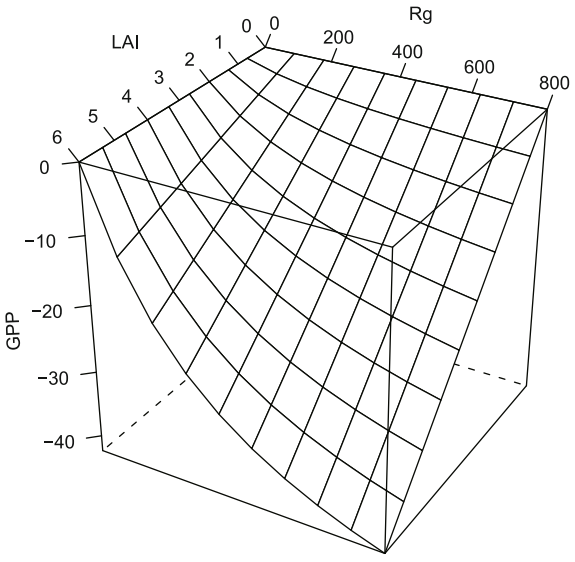

Figure 3 Leaf-light response of GPP in the potato field according to eq. (6). GPP is given in μmol CO_2 m^{-2} s^{-1}, LAI given in m^2 m^{-2}, and R_g in W m^{-2}.

ear relationship between α (or β) and active LAI, and that the difference in the light use efficiency between crops is likely due to the individual value of α' for each crop. Lindner et al. (2015) suggested that this relationship is possibly due to increased chlorophyll in the growing leaves. Their conclusions, that the solar radiation controls the diurnal patters in GPP and NEE, while the changing α and LAI controls the seasonal patterns, can be consistently explained by our leaf-light response function.

The LAI-factor scheme has the following advantages, conferred by using the whole Database-parameterization without any grouping. Firstly, conventional gap-filling methods suffer from a lack of data in each data class, if the width of time windows or temperature classes (mean diurnal variance method and non-linear regression method) or the width of the cells (look-up table method) does not match the statistical data distribution. The conflict exists in the requirement for a time-window to be short enough to exclude the errors contained in the nonlinear dependence of environmental variables (Falge et al., 2001) and to be long enough to contain sufficient data for calculating a meaningful statistic needed to apply the mean diurnal variance method, the look-up table method, or the non-linear regression method. This statistical problem can be avoided by using the LAI-factor scheme. Secondly, the time-window related schemes have difficulties if large gaps exist, and fail when the period of the missing data is longer than the time-window itself (Stoy et al., 2006). These cases often occur due to the power failure at the locations of field campaigns or during longer rain or fog events (e.g. in the monsoon and subsequent typhoon season in South Korea). Conventionally, the time-window scheme could fill these large gaps by interpolating the parameters or the fluxes calculated before and after the gaps. Unfortunately, it could introduce errors when the LAI develops non-linearly in time. For instance, if a gap takes place during the period at the maximum of the LAI when the potential photosynthesis ability reaches the maximal efficiency, this simple interpolation will underestimate the GPP. The LAI-factor scheme can overcome this problem if the LAI is available during these large gaps.

Errors in the estimation of LAI could have influence on the performance of the LAI-factor scheme. Every measured LAI-value in our case was estimated from several randomly sampled plants in the footprint-area of the eddy-covariance measurement of both field sites. Since individual plants develop differently from each other, the limited number of samples could result in an error through the calculation of a representative mean. Furthermore, the simple linear interpolation to fill the time-steps between the distinct LAI measurements could miss some development stages of the plants. LAI normally remains constant at a potato field when the crop is fully developed (González-Sanpedro et al., 2008). Unfortunately, during our field campaign only one measurement at the growing peak during the mid-season stage was available (Figure 1). Thus, the linear interpolation could probably underestimate the real LAI before and after the peak value. Finally, during the mid-seasons when LAI is large, the overlapping of green leaves results in less effective photosynthesis than during the early and late seasons, which makes the estimated mid-season LAI larger than the effective LAI (so called foliar clumping effect). These potential errors mentioned above could explain why the time-window scheme with small time windows sometimes performs better than the LAI-factor scheme. It could be expected that a better estimation of effective LAI would improve the performance of the LAI-factor scheme. A large amount of manual biomass sampling could possibly improve the parameterization of daytime NEE, but this sampling method is destructive and thus could change the footprint of the eddy-covariance measurement. Satellite imaging (González-Sanpedro et al., 2008, resolution of 30 m; Jiang et al., 2010, resolution of 1 km), camera retrieving (Migliavacca et al., 2011) or modeling (Li et al., 2011) could be alternatives and expected to reduce these errors and improve the simulation.

3.4 Temperature-binning scheme

The performances of temperature-binning approaches are shown in Figure 4. All the temperature-binning approaches (class widths between 28 and 2 K) for the potato field have a poor performance, with low indexes of agreement (d < 0.72) and low NSeff < 0.32. The consequently reduced class widthonly slightly improves the explained variance for NEEfor the potato field, which proves a poor sensitivity of the potatoes to temperature. However, for the rice field, d increases from 0.61 to 0.85 and NSeff from 0.16 to 0.58, decreasing the width of the temperature bins from 28 to 8 K, which superficially indicates a better temperature sensitivity of the rice.

For both sites, the smaller classes of 8, 4 and 2 K have a similar performance, indicating that it is unnecessary to bin the data into temperature classes smaller than 8 K. This range is larger than the 4 K temperature class used by Falge et al. (2001) for a variety of sites including croplands and the 2 K temperature class used by Ruppert et al. (2006) for a forest site. They also reported that additional time windows do not significantly improve the temperature binning method, because the existing long-time seasonal temperature response of the long-living and slow-growing coniferous forest is already covered by the time-independent allocation of the values into the temperature bins. However, this could fail for short-living and fast-growing crops, thus we found that the temperature-binning scheme and time-window scheme perform differently in our study. Either the LAI-factor scheme or the time-window scheme, even with the 16 d time-window approach, results in a much better agreement than the smallest temperature binning (2 K) approach. This implies that, if

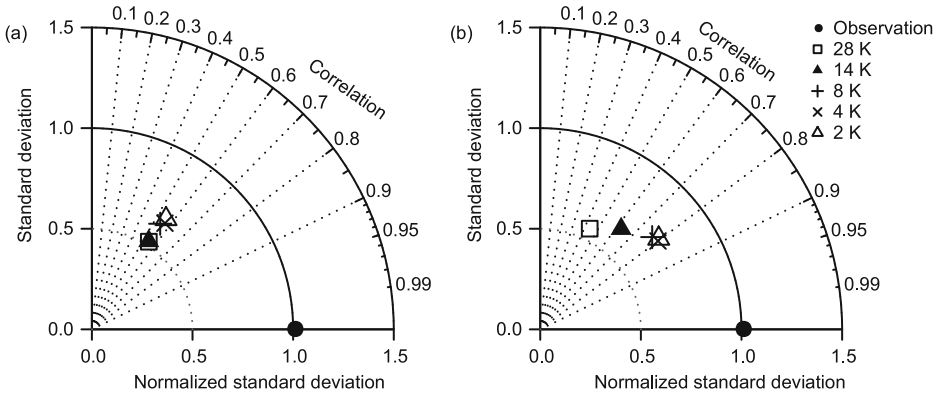

Figure 4 Taylor diagrams for the performances of simulations applying the temperature binning scheme at the potato field (a) and the rice field (b). The polar radial distance is the normalized standard deviation (NSD). The polar angle is the correlation coefficient (*R*).

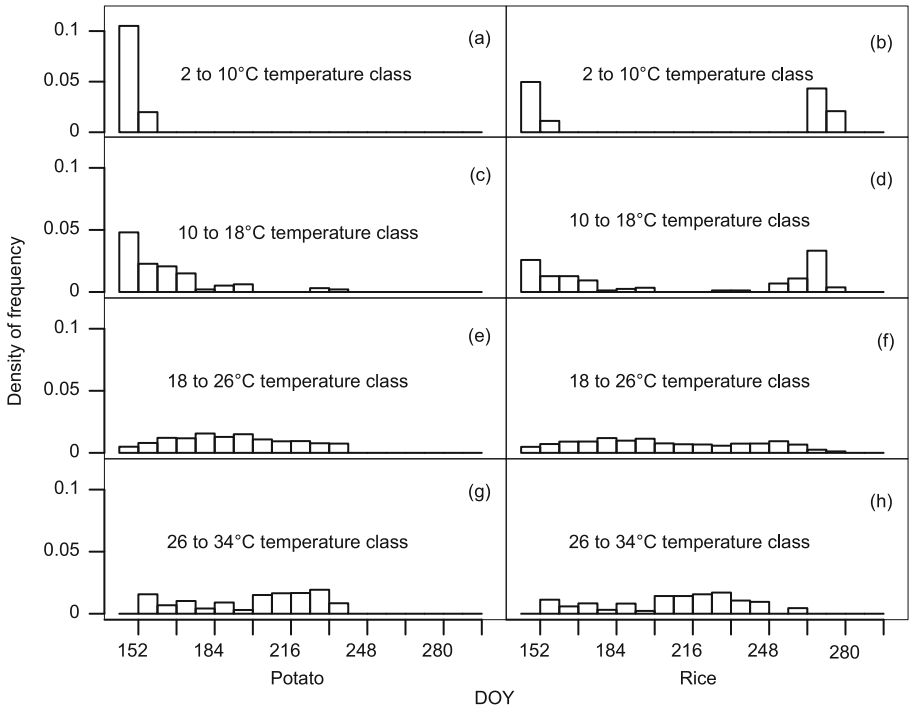

Figure 5 Temporal distribution of temperature measurements within temperature classes at the potato field and the rice field.

the seasonal or daily weather conditions are in a normal climate range, the long-time seasonal and short time diurnal temperature responses of the crops play a minor role compared to the fast changing development of the crop plant. Furthermore, we combined the LAI-factor scheme with the temperature binning approach. We found that additional temperature binning does not improve the simulation of the LAI-factor scheme (not shown), which demonstrates that the temperature dependency can be ignored if the plant development is well considered. The temporal distribution within temperature classes (Figure 5) could explain why a smaller temperature binning could improve the simulation for both sites in spite of the minor temperature dependency. Some temperature values were observed only during some special periods. For instance, the 2 to 10°C temperature class at the potato field falls exactly into the DOY 144 to 160 time window, which makes the overall simulation of the 8 K temperature binning approach better than the simulation of larger temperature classifications. Since the 18–26°C temperature class is distributed over almost the whole growing season, the temperature binning scheme mixes these time windows together and fails to perform a good simulation.

The application of temperature-binning scheme has been less common than the time window scheme in the recent years, but the reason has not been explained in the literature. According to our study, temperature binning contains some, but not all, relevant information of seasonal response for NEE gap-filling for croplands, which is insufficient for the regression of the light response function. The air temperature has both a diurnal and a seasonal cycle within a year. As the diur-

nal cycle of temperature is partly a function of solar radiation, which is included in the light response function, and the seasonal cycle of temperature is contained in the time-window scheme or the LAI-factor scheme, we suggest that temperature binning could be ignored if the plant development is well simulated.

3.5 VPD factor

The asymmetric pattern in the diurnal cycle of NEE should be considered in gap-filling because in the afternoon higher temperature and higher VPD leads to a higher evaporation rate and then to a stomatal closure (Lasslop et al., 2010). We used the time-window scheme including a VPD-factor to test this effect on the irrigated and non-irrigated croplands. The VPD effect on the rice field can be ignored during the whole-growing season (Figure 6b), because with the permanently irrigated and flooded rice terraces, the observed VPD is below the plant physiological threshold (VPD_0 = 10 hPa) during most of time of the growing season (Figure 7). At the non-irrigated potato field, the VPD-effect can be ignored during the active monsoon, but must be taken into account during pre-monsoon season (e.g. DOY 152 to 175, Figure 7), especially in the afternoon when the VPD exceeded 15 hPa (Figure 6a), because of dry weather. These high VPD values during this pre-monsoon period can have a significant impact to the gap-filling of the whole growing season depending on the length of the dry pre-monsoon period compared to the total growing season.

3.6 Step-by-step gap-filling scheme

Based on the results of the previous sections, we defined an

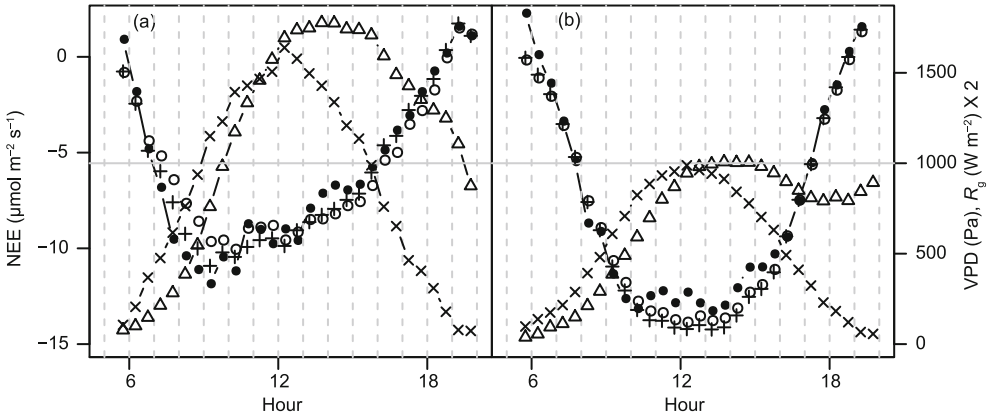

Figure 6 Mean diurnal cycles of vapor pressure deficit (VPD, △), solar radiation (×), observed NEE (●), simulated NEE by the time-window scheme without VPD-factor (○) and with VPD-factor (+) for the potato field during the earlier growing season (a) and the rice field during the whole season (b).

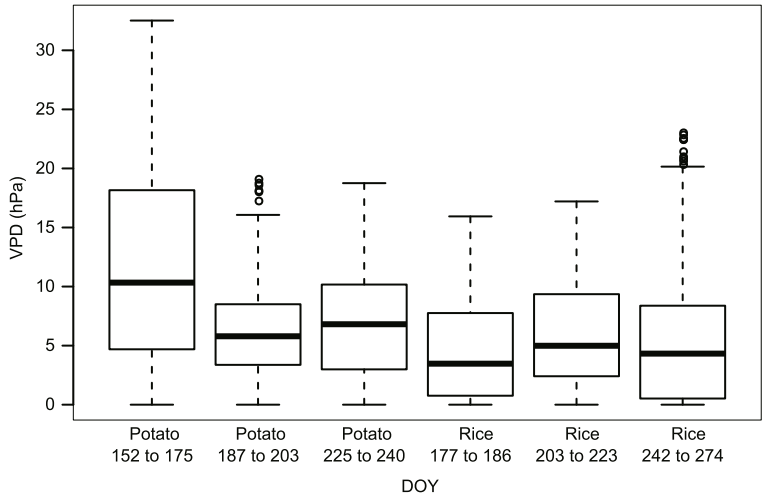

Figure 7 Boxplot of vapor pressure deficit (VPD) during each measurement period at the potato field and the rice field. The boxplot is composed of the median (solid line), the lower quartile and upper quartile (i.e. the 25th and 75th percentile, box), the lowest datum still within 1.5 times of interquartile range (IQR) of the lower quartile, and the highest datum still within 1.5 IQR of the upper quartile (markers).

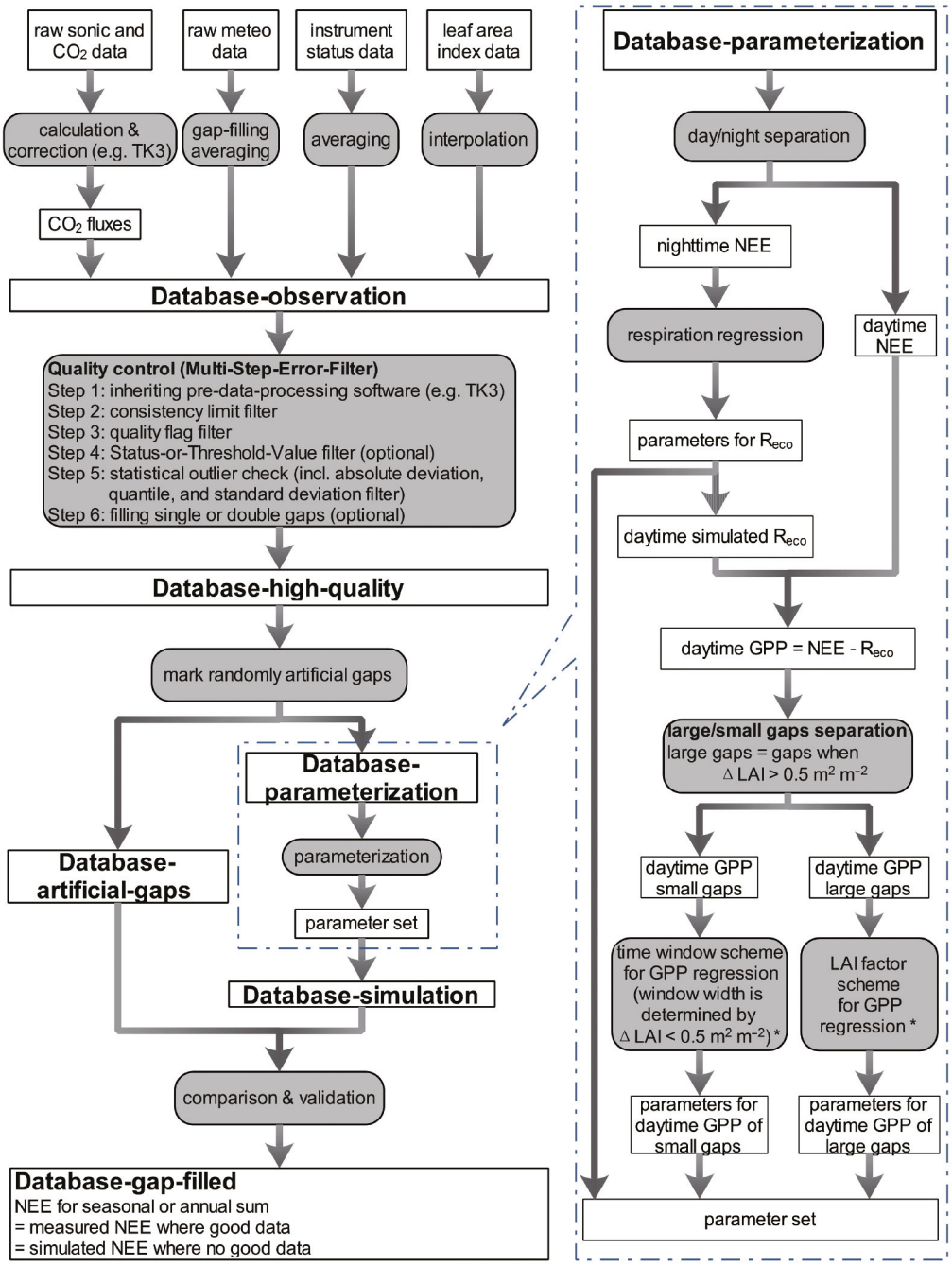

Figure 8 Scheme of data-processing for the calculation of annual sums of NEE, partly based on the scheme by Ruppert et al. (2006). Rectangular boxes represent datasets. Rounded boxes represent data processing steps. The compensation of vapor pressure deficit (VPD) can be inserted into the positions marked with "*". The abbreviations stand for eddy-covariance software package of the Department of Micrometeorology, University of Bayreuth (TK3), the Net Ecosystem Exchange (NEE), Gross Primary Production (GPP), ecosystem Respiration (R_{eco}), and Leaf Area Index (LAI).

overall step-by-step scheme for helping to determine NEE of CO_2 of fast-growing croplands, which is presented in Figure 8.

4. Conclusions

Based on the conventional light response function, the new leaf-light response function suggested in this study can be used as a new gap-filling scheme with a LAI-factor for croplands. It features the inclusion of the vegetation status information rather than the simple linear interpolation of NEE, and the use of the whole data-set for parameterization. These features have advantages for short-living fast-growing croplands, especially for those suffering from the lack of observation resulted from bad weather, power failure, patchy planting, and intensive farmland managements. Although the con-

ventional time window approach is still the best data binning scheme for the non-linear regression method if sufficient observation is available within each time window, a seasonal or monthly time window could significantly decline the performance of the simulation. We found the optimal window width is four days for potatoes and eight days for rice. Within these window widths the mean value of ΔLAI is 0.5 m^2 m^{-2}, which could be a reference to determine the time window width for other fast-changing vegetation surfaces. On the other hand, the seasonal response cannot be captured by the conventional time-independent temperature binning approach, which should be ignored. The VPD effect above irrigated agriculture (e.g. rice) in East-Asia can be ignored during the whole growing season. At the non-irrigated cropland (e.g. potato, carrot or cabbage), the VPD-effect can be ignored during the active monsoon but must be taken into account during pre-monsoon season. Since the humidity conditions of non-irrigated croplands are quite site-specific, the VPD influence should be checked for different sites. In general, we recommend using the conventional time-window scheme together with our new LAI-factor scheme to fill gaps in the NEE time series for fast-growing croplands. These two schemes have the advantages of treating small and large gaps, respectively.

Acknowledgements *We deeply thank Thomas Foken for his helpful comments. We also thank John Tenhunen for the major support without which this work would not be possible. We are very thankful for the help of all the South Korean and German fellow PhD students, especially Bora Lee and Steve Lindner, during the field operation in Korea. We also appreciate the help given by the colleagues of the Department of Micrometeorology and Department of Plant Ecology, University of Bayreuth. This study was carried out as part of the International Research Training Group TERRECO (Grant No. GRK 1565/1) funded by the Deutsche Forschungsge-meinschaft (DFG) at the University of Bayreuth, Germany and the Korean Research Foundation (KRF) at Kangwon National University, Chuncheon, South Korea.*

References

Ammann C, Flechard C, Leifeld J, Neftel A, Fuhrer J. 2007. The carbon budget of newly established temperate grassland depends on management intensity. Agric Ecosyst Environ, 121: 5–20

Baldocchi D D. 2003. Assessing the eddy covariance technique for evaluating carbon dioxide exchange rates of ecosystems: Past, present and future. Glob Change Biol, 9: 479–492

Baldocchi D, Falge E, Gu L, Olson R, Hollinger D, Running S, Anthoni P, Bernhofer C, Davis K, Evans R, Fuentes J, Goldstein A, Katul G, Law B, Lee X, Malhi Y, Meyers T, Munger W, Oechel W, Paw K T, Pilegaard K, Schmid H P, Valentini R, Verma S, Vesala T, Wilson K, and Wofsy S. 2001. FLUXNET: A new tool to study the temporal and spatial variability of ecosystem-scale carbon dioxide, water vapor, and energy flux densities. Bull Amer Meteorol Soc, 82: 2415–2434

Bassow S L, Bazzaz F A. 1998. How environmental conditions affect canopy leaf-level photosynthesis in four deciduous tree species. Ecology, 79: 2660–2675

Béziat P, Ceschia E, Dedieu G. 2009. Carbon balance of a three crop succession over two croplandsites in South West France. Agric For Meteorol, 149: 1628–1645

Du Q, Liu H. 2013. Seven years of carbon dioxide exchange over a degraded grassland and a cropland with maize ecosystems in a semiarid area of China. Agric Ecosyst Environ, 173: 1–12

Eigenmann R, Kalthoff N, Foken T, Dorninger M, Kohler M, Legain D, Pigeon G, Piguet B, Schüttemeyer D, Traulle O. 2011. Surface energy balance and turbulence network during COPS. Q J R Meteorol Soc, 137: 57–69

Falge E, Baldocchi D, Olson R, Anthoni P, Aubinet M, Bernhofer C, Burba G, Ceulemans R, Clement R, Dolman H, Granier A, Gross P, Grunwald T, Hollinger D, Jensen N O, Katul G, Keronen P, Kowalski A, Lai C T, Law B E, Meyers T, Moncrieff H, Moors E, Munger J W, Pilegaard K, Rannik U, Rebmann C, Suyker A, Tenhunen J, Tu K, Verma S, Vesala T, Wilson K, Wofsy S. 2001. Gap filling strategies for defensible annual sums of net ecosystem exchange. Agric For Meteorol, 107: 43–69

Falge E, Baldocchi D, Tenhunen J, Aubinet M, Bakwin P, Berbigier P, Bernhofer C, Burba G, Clement R, Davis K J, Elbers J A, Goldstein A H, Grelle A, Granier A, Guomundsson J, Hollinger D, Kowalski A S, Katul G, Law B E, Malhi Y, Meyers T, Monson R K, Munger J, Oechel W, Paw U K T, Pilegaard K, Rannik Ü, Rebmann C, Suyker A, Valentini R, Wilson K, Wofsy S. 2002. Seasonality of ecosystem respiration and gross primary production as derived from FLUXNET measurements. Agric For Meteorol, 113: 53–74

Foken T, Wichura B. 1996. Tools for quality assessment of surface-based flux measurements. Agric For Meteorol, 78: 83–105

Foken T, Göckede M, Mauder M, Mahrt L, Amiro B D, Munger J W. 2004. Post-field data quality control. In: Lee X, Massman W J, Law B, eds. Handbook of Micrometeorology: A Guide for Surface Flux Measurement and Analysis. Dordrecht: Kluwer. 181–208

González-Sanpedro M C, Le Toan T, Moreno J, Kergoat L, Rubio E. 2008. Seasonal variations of leaf area index of agricultural fields retrieved from Landsat data. Remote Sens Environ, 112: 810–824

Gove J, Hollinger D. 2006. Application of a dual unscented Kalman filter for simultaneous state and parameter estimation in problems of surface-atmosphere exchange. J Geophys Res, 111: D08S07

Greco S, Baldocchi D D. 1996. Seasonal variations of CO_2 and water vapour exchange rates over a temperate deciduous forest. Glob Change Biol, 2: 183–197

Hui D, Wan S, Su B, Katul G, Monson R, Luo Y. 2004. Gap-filling missing data in eddy covariance measurements using multiple imputation (MI) for annual estimations. Agric For Meteorol, 121: 93–111

Jiang B, Liang S, Wang J, Xiao Z. 2010. Modeling MODIS LAI time series using three statistical methods. Remote Sens Environ, 114: 1432–1444

Kwon H, Kim J, Hong J, Lim J H. 2010. Influence of the Asian monsoon on net ecosystem carbon exchange in two major ecosystems in Korea. Biogeosciences, 7: 1493–1504

Lasslop G, Reichstein M, Papale D, Richardson A D, Arneth A, Barr A, Stoy P, Wohlfahrt G. 2010. Separation of net ecosystem exchange into assimilation and respiration using a light response curve approach: Critical issues and global evaluation. Glob Change Biol, 16: 187–208

Legates D R, McCabe G J. 1999. Evaluating the use of "goodness-of-fit" measures in hydrologic and hydroclimatic model validation. Water Resour Res, 35: 233–241

Lei H M, Yang D W. 2010. Seasonal and interannual variations in carbon dioxide exchange over a cropland in the North China Plain. Glob Change Biol, 16: 2944–2957

Li L, Vuichard N, Viovy N, Ciais P, Wang T, Ceschia E, Jans W, Wattenbach M, Béziat P, Gruenwald T, Lehuger S, Bernhofer C. 2011. Importance of crop varieties and management practices: Evaluation of a process-based model for simulating CO_2 and H_2O fluxes at five European maize (*Zea mays* L.) sites. Biogeosciences, 8: 1721–1736

Lindner S, Otieno D, Lee B, Xue W, Arnhold S, Kwon H, Huwe B, Tenhunen J. 2015. Carbon dioxide exchange and its regulation in the main agro-ecosystems of Haean catchment in South Korea. Agric Ecosyst Environ, 199: 132–145

Lloyd J, Taylor J A. 1994. On the temperature dependence of soil respiration. Funct Ecol, 8: 315–323

Lüers J, Detsch F, Zhao P. 2014. Application of a multi-step error filter for post-processing atmospheric flux and meteorological basic data. Work Report 58. Bayreuth: University of Bayreuth, Department of Micrometeorology

Mauder M, Foken T. 2011. Documentation and instruction manual of the eddy covariance software package TK3. Work Report 46. Bayreuth: University of Bayreuth, Department of Micrometeorology

Mauder M, Liebethal C, Göckede M, Leps J P, Beyrich F, Foken T. 2006. Processing and quality control of flux data during LITFASS-2003. Bound Lay Meteorol, 121: 67–88

Mauder M, Oncley S P, Vogt R, Weidinger T, Riberio L, Bernhofer C, Foken T, Kohsiek W, DeBruin H, Liu H. 2007. The energy balance experiment EBEX-2000. Part II: Intercomparison of eddy covariance sensors and post-field data processing methods. Bound Lay Meteorol, 123: 29–54

Mauder M, Foken T, Clement R, Elbers J A, Eugster W, Grünwald T, Heusinkveld B, and Kolle O. 2008. Quality control of CarboEurope flux data—Part 2: Inter-comparison of eddy-covariance software. Biogeosciences, 5: 451–462

Michaelis L, Menten M. 1913. Die Kinetik der Invertinwirkung. Biochem Z, 49: 333–369

Migliavacca M, Galvagno M, Cremonese E, Rossini M, Meroni M, Sonnentag O, Cogliati S, Manca G, Diotri F, Busetto L, Cescatti A, Colombo R, Fava F, Morra di Cella U, Pari E, Siniscalco C, Richardson A. 2011. Using digital repeat photography and eddy covariance data to model grassland phenology and photosynthetic CO_2 uptake. Agric For Meteorol, 151: 1325–1337

Millennium Ecosystem Assessment. 2005. Ecosystems and Human Wellbeing: Synthesis. Washington, DC: Island Press

Moffat A M, Papale D, Reichstein M, Hollinger D Y, Richardson A D, Barr A G, Beckstein C, Braswell B H, Churkina G, Desai A R, Falge E, Gove J H, Heimann M, Hui D, Jarvis A J, Kattge J, Noormets A, Stauch V J. 2007. Comprehensive comparison of gap-filling techniques for eddy covariance net carbon fluxes. Agric For Meteorol, 147: 209–232

Oncley S P, Foken T, Vogt R, Kohsiek W, DeBruin H, Bernhofer C, Christen A, van Gorsel E, Grantz D, Feigenwinter C, Lehner I, Liebethal C, Liu H, Mauder M, Pitacco A, Riberio L, Weidinger T. 2007. The energy balance experiment EBEX-2000. Part I: Overview and energy balance. Bound Lay Meteorol, 123: 1–28

Otieno D, Wartinger M, Nishiwaki A, Hussain M, Muhr J, Borken W, Lischeid G. 2009. Responses of CO_2 exchange and primary production of the ecosystem components to environmental changes in a mountain peatland. Ecosystems, 12: 590–603

Papale D. 2012. Data gap filling. In: Aubinet M, Vesala T, Papale D eds. Eddy Covariance: A Practical Guide to Measurement and Data Analysis. Dordrecht, Heidelberg, London, New York: Springer. 159–172

Papale D, Valentini R. 2003. A new assessment of European forests carbon exchanges by eddy fluxes and artificial neural network spatialization. Glob Change Biol, 9: 525–535

Papale D, Reichstein M, Aubinet M, Canfora E, Bernhofer C, Kutsch W, Longdoz B, Rambal S, Valentini R, Vesala T, Yakir D. 2006. Towards a standardized processing of Net Ecosystem Exchange measured with eddy covariance technique: Algorithms and uncertainty estimation. Biogeosciences, 3: 571–583

Reichstein M, Falge E, Baldocchi D, Papale D, Aubinet M, Berbigier P, Bernhofer C, Buchmann N, Gilmanov T, Granier A, Grunwald T, Havrankova K, Ilvesniemi H, Janous D, Knohl A, Laurila T, Lohila A, Loustau D, Matteucci G, Meyers T, Miglietta F, Ourcival J M, Pumpanen J, Rambal S, Rotenberg E, Sanz M, Tenhunen J, Seufert G, Vaccari F, Vesala T, Yakir D, Valentini R. 2005. On the separation of net ecosystem exchange into assimilation and ecosystem respiration: Review and improved algorithm. Glob Change Biol, 11: 1424–1439

Richardson A D, Hollinger D Y. 2007. A method to estimate the additional uncertainty in gap-filled NEE resulting from long gaps in the CO_2 flux record. Agric For Meteorol, 147: 199–208

Ruppert J, Mauder M, Thomas C, Lüers J. 2006. Innovative gap-filling strategy for annual sums of CO_2 net ecosystem exchange. Agric For Meteorol, 138: 5–18

Saxe H, Cannell M G R, Johnsen Ø, Ryan M G, Vourlitis G. 2001. Tree and forest functioning in response to global warming. New Phytol, 149: 369–399

Stoy P C, Katul G G, Siqueira M, Juang J Y, Novick K A, Uebelherr J M, Oren R. 2006. An evaluation of models for partitioning eddy covariance-measured net ecosystem exchange into photosynthesis and respiration. Agric For Meteorol, 141: 2–18

Suyker A E, Verma S B, Burba G G, Arkebauer T J. 2005. Gross primary production and ecosystem respiration of irrigated maize and irrigated soybean during a growing season. Agric For Meteorol, 131: 180–190

Taylor K E. 2001. Summarizing multiple aspects of model performance in a single diagram. J Geophys Res, 106: 7183–7192

Xing Z, Bourque C P A, Meng F, Zha T, Cox R M, Swift D E. 2007. A simple net ecosystem productivity model for gap filling of tower-based fluxes: An extension of Landsberg's equation with modifications to the light interception term. Ecol Model, 206: 250–262

Zhao P, Lüers J, Olesch J, Foken T. 2011. Documentation of the observation period, 12 May to 8 November 2010, Haean, South Korea. Work Report 45. Bayreuth: University of Bayreuth, Department of Micrometeorology